Geoderma 343 (2019) 60–71

Contents lists available at ScienceDirect

Geoderma

journal homepage: www.elsevier.com/locate/geoderma

Soil organic carbon and soil erosion – Understanding change at the large catchment scale

G.R. Hancock[a,*], V. Kunkel[a], T. Wells[b], Cristina Martinez[c]

[a] School of Environment and Life Sciences, The University of Newcastle, Australia
[b] School of Engineering, The University of Newcastle, Australia
[c] School of Agriculture and Food Sciences, The University of Queensland, Australia

ARTICLE INFO

Handling Editor: Alex McBratney

Keywords:
Soil organic carbon
Carbon cycle
Soil erosion
Environmental tracers
Climate change

ABSTRACT

Soil organic carbon (SOC) is a major soil component. However, there is still much to learn regarding its spatial and temporal distribution as well as how SOC moves through the landscape. Of particular interest is how SOC movement is related to soil erosion and deposition. Here we examine the spatial distribution of SOC over two large (562 and 606 km^2) catchments in relation to soil erosion and deposition. We found that the spatial distribution of SOC concentration on average is stable (over an eight year period) for the two study catchments. However, differences were found in SOC when concentrations were compared between samples collected in 2006 and 2014. The environmental tracer caesium-137 (^{137}Cs) was used to assess erosion and deposition patterns across the study catchment and a significant relationship was found between SOC change and erosion and deposition at each sample point. That is, locations with an increase in SOC corresponded with an increase in ^{137}Cs concentration (depositional sites) while locations with a decrease in SOC corresponded with a decrease in ^{137}Cs concentration (erosional sites). A Monte-Carlo assessment confirmed these results. The driver of the SOC change and soil movement corresponds with the largest rainfall event (since 1969) in the area. The results suggest that SOC can be translocated by significant rainfall events. The findings provide insight into how catchments may respond to stronger and more frequent storm events.

1. Introduction

It is well recognised that the interaction of atmospheric CO_2 with terrestrial carbon (C) storage is one of the largest and most uncertain feedbacks of the carbon cycle (Schimel et al., 2015). This uncertainty is due to the complex interactions among several biophysical and hydroclimatic processes that drive soil organic carbon (SOC) distribution, including the dynamics of rainfall, soil moisture, and insolation, together with soil erosion and deposition (Lal, 2004; Kirkels et al., 2014; Doetterl et al., 2016).

With the global soil resource containing 2300 Gt C and holding more C than the atmosphere (800 Gt) and vegetation (550 Gt) combined, a small variation in soil C may change atmospheric CO_2 concentration (Luo et al., 2010; Hoyle et al., 2016; Nadeu et al., 2015; Minasny et al., 2018). Therefore, understanding and quantifying SOC and its movement is of key importance for both soil conservation and atmospheric CO_2 mitigation strategies, such as C sequestration (Fig. 1). This has resulted in a demand for a more accurate mapping of the soil C pool at higher resolution (Minasny et al., 2013).

Understanding the spatiotemporal distribution of SOC and its dynamic changes will allow better prediction of climate change impacts as well as being necessary for understanding the soil C inventory to enhance soil C sequestration (Quinton et al., 2010; Dorji et al., 2014; Kirkels et al., 2014; Nadeu et al., 2015; Doetterl et al., 2016). A key issue is the difficulty of quantifying SOC spatial and temporal change as knowledge is needed both at site-specific plot-scales as well as large spatial scales.

The carbon cycle and its relationship with soil and topography is complex (Fig. 1). Catenary soil development and soil patterns together with terrain attributes can help characterize SOC spatio-temporal patterns. SOC patterns in the landscape are strongly influenced by the distribution of water and soil (Jenny, 1941; Moore et al., 1993; Pennock and Corre, 2001; Mueller and Pierce, 2003), therefore it is likely that SOC can be predicted from topography or terrain parameters that help characterize flow paths (Oueslati et al., 2013; Kunkel et al., 2019). Explicit relationships and models that link landscape and topographic characteristics with SOC processes are needed (Fissore et al., 2017) (Fig. 1). Since the development of digital soil mapping technologies in

* Corresponding author.
E-mail address: greg.hancock@newcastle.edu.au (G.R. Hancock).

https://doi.org/10.1016/j.geoderma.2019.02.012
Received 31 October 2018; Received in revised form 1 February 2019; Accepted 4 February 2019
Available online 22 February 2019
0016-7061/

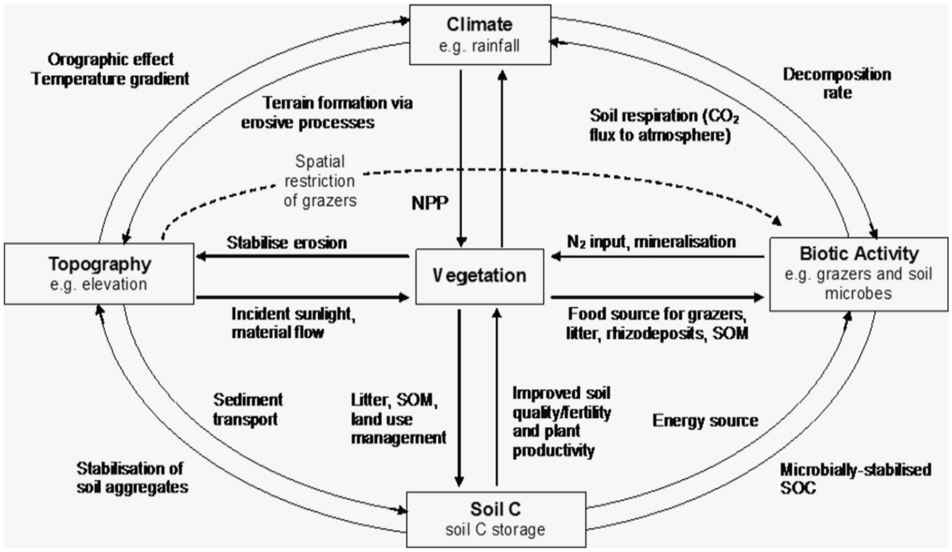

Fig. 1. Conceptual diagram showing abiotic and biotic controls on SOC, and their potential feedbacks.

the late 1990s, and formalization of the discipline by McBratney et al. (2003), mapping of soil C at the field and regional scales has become an area of active research (Minasny et al., 2013). However, a unifying model that captures topography and climate together with soil properties (soil physics, soil chemistry and soil biology) to predict the spatio-temporal distribution of SOC is yet to be developed.

Soil erosion can lead to soil degradation and loss of soil structure, soil nutrients and SOC (Pimentel et al., 1995; Gregorich et al., 1998; Lal, 2003, 2004). Soil erosion plays an important role in the re-distribution of soil C, particularly C that is strongly bound to soil aggregates (Fig. 1). Further, there is a well-recognised and debated relationship between soil erosion and deposition and SOC (Moore et al., 1993; Lal, 2001, 2003; Hancock et al., 2010b; Quinton et al., 2010). That is, the decomposition of old SOC and the sequestration and stabilization of fresh SOC input that occur simultaneously at any site (Berhe et al., 2007, 2008; Kirkels et al., 2014; Doetterl et al., 2016; Berhe et al., 2014). Soil erosion is a naturally occurring three stage process involving detachment, transportation, and deposition (Pimentel et al., 1995; Lal, 2001; Poesen, 2018). However, there is growing concern that climate change and/or enhanced climate variability will increase erosion, thus questions surround how this will affect the distribution of SOC. Of particular interest is how an increase in storm frequency and intensity may influence soil erosion and deposition as well as SOC distribution and ultimately the hillslope and catchment C balance (Poesen, 2018). This is particularly important as many climate models predict a future increase in storm frequency and intensity (such as the current study site) (CSIRO, 2016).

Erosive forces can be highly selective, leaving behind larger particles due to the required force to entrain them and finer particles due to their cohesiveness. The particles least resistant to erosive forces are clay, silt and fine sand. Erosion of this material leads to the preferential loss of soil organic matter (SOM) and changes in particle size distribution (Lal, 2001, 2003; Morgan, 2009). The higher SOC concentrations in depositional profiles are usually related to the preferential detachment and downslope transport of the more labile, and lighter, soil fractions which are typically enriched in C, relative to the bulk soil (Doetterl et al., 2012; Kirkels et al., 2014). How much SOC is transported by soil erosion is a much debated topic (Kuhn, 2010; Quinton et al., 2010; Hu and Kuhn, 2014).

There are many different field and laboratory based methods available to researchers for measuring or quantifying soil erosion rates (Toy et al., 2002; Hancock and Lowry, 2015; Lal, 2001; Poesen, 2018). This study investigates the spatiotemporal distribution of surface SOC concentrations and its relationship with erosion and deposition across two large (~600 and ~700 km^2) catchments with similar geomorphology, climate, soils, vegetation and land-use. Here, we use the artificial radioisotope ^{137}Cs, as a temporal erosion-deposition tracer at a study site in south-east Australia. ^{137}Cs, the by-product of the atmospheric testing of nuclear weapons, is as well-understood and proven method, which has been extensively employed globally and in Australia. Zapata (2002) and Zapata et al. (2002) provide a thorough background on the technique and its use to determine erosion and deposition patterns and rates as well as many others (Loughran, 1994; Loughran et al., 2002, 2004; Kirchner, 2013; Poreba, 2006; Ritchie and McHenry, 1975, 1990).

There are significant questions regarding the relationship between soil erosion and SOC movement. Previous work by the authors has shown that there was a significant increase in erosion after a major rainfall event at the current study site (Hancock and Coulthard, 2012; Hancock et al., 2015). There are significant questions surrounding how the landscape will respond to a change in climate forcing in many parts of the world including south-east Australia (Verdon-Kidd et al., 2014; CSIRO, 2016).

The work here forms part of a long-term investigation of hydrology, sediment transport and soil properties in the south-east region of Australia (Martinez et al., 2007; Martinez et al., 2009; Martinez et al., 2010a, 2010b; Rüdiger et al., 2007; Hancock et al., 2010a, 2010b, 2011, 2015; Hancock and Coulthard, 2012; Wells et al., 2013; Chen et al., 2015; Kunkel et al., 2016, 2019). This study will (1) assess the large catchment-scale spatiotemporal distribution of SOC for two geomorphologically similar catchments for two different time periods and its relationship with erosion and deposition; and (2) assess the relationship between SOC and soil erosion and deposition.

2. Site description

The Krui (562 km^2) and Merriwa (606 km^2) River catchments are located within the Goulburn River catchment (6540 km^2), in the Hunter Valley region of New South Wales, Australia (Fig. 2). The catchments have six (Krui catchment) and seven (Merriwa catchment) permanently instrumented weather stations which record rainfall, air and soil temperature as well as soil moisture at different depths (Rüdiger et al., 2007; Kunkel et al., 2016) (Table 1). The sites have been operating since 2003 with longer term rainfall data supplemented by Bureau of Meteorology data (www.bom.gov.au).

The study site is bounded to the north by the Liverpool Ranges,

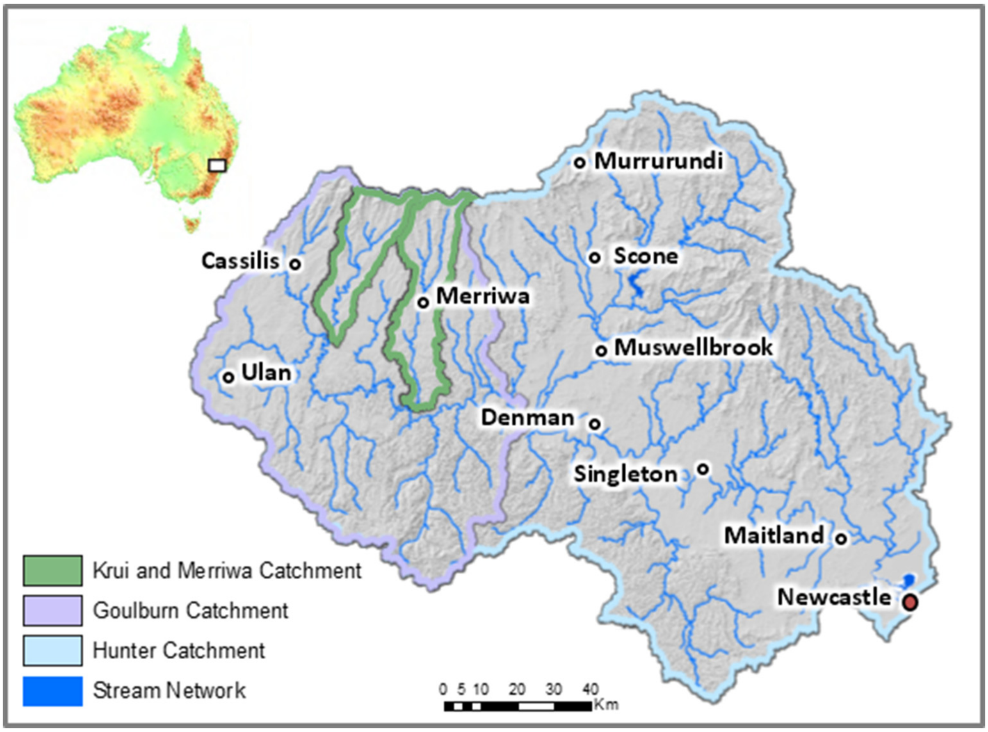

Fig. 2. Location map of Krui and Merriwa River catchments (green outline), Goulburn River catchment (purple outline) and Hunter River catchment (blue outline). (For interpretation of the references to colour in this figure legend, the reader is referred to the web version of this article.)

Table 1
Key site parameters for Krui and Merriwa weather station sites.

Krui sites	K1	K3	K4	K5	K6
Elevation (m)	386	404	411	459	739
Slope (°)	2	1	14	4	17
Aspect (°)	77	331	147	120	116
Soil depth (cm)	> 90	> 90	> 90	> 90	> 90
Soil type	Silt loam	Clay	Clay	Clay	Clay loam
Land cover	Crop/ fallow	Crop/ fallow	Native pasture	Native pasture	Improved pasture

Merriwa sites	M3	M4	M5	M6	M7
Elevation (m)	419	340	362	391	516
Slope (°)	3	6	5	4	12
Aspect (°)	296	163	101	289	138
Soil depth (cm)	60–90	30–60	60–90	60–90	> 90
Soil type	Clay-loam	Loam	Clay	Clay	Clay-loam
Land cover	Native pasture	Native pasture	Native pasture	Native pasture	Improved pasture

where topography is rugged, while the landscape to the south, around Merriwa and Cassilis, is hilly to undulating (Story et al., 1963). Elevations for both catchments range from approximately 200 m in the south (Merriwa Plateau) to 1200 m in the north (Liverpool Range). The catchments are underlain with Tertiary basalt of the Liverpool Range beds and forms part of the Merriwa Plateau (Story et al., 1963). Older sedimentary sequences which are Jurassic - Triassic in age are exposed to the south of the study site. The Krui and Merriwa catchments are considered to be geomorphologically similar (Kunkel et al., 2016).

The study site is located in the temperate zone of eastern Australia. Climate in the region is dominated by a continental influence, although topography, elevation and proximity to the ocean are also considered important. Monthly rainfall data for the region are 50–60 mm in summer and 30–40 mm in winter, where winter rainfall is least variable, and rainfall in late summer-autumn is most variable (Kovac and Lawrie, 1991). Annual average rainfall is highest in the north near the Liverpool Ranges (approximately 1000 mm), and decreases gradually upon moving southwards to the Merriwa Plateau (approximately 500 mm). Annual rainfall was lower in 2006, compared to 2014 and 2015 (Fig. 3). There are also two years with high rainfall erosivity values as calculated by Renard and Freimund (1994) based on rainfall data from 1969 onwards (www.bom.gov.au). Of particular note is a storm in 2007, which was the largest on record (since 1969).

The monthly mean minimum and maximum air temperatures are 3 °C (winter) and 16 °C (summer), and 17 °C (winter) and 30 °C (summer) respectively (Australian Bureau of Meteorology, 1988).

Much of the original vegetation in the region has been cleared, the extent of which has largely been influenced by topography. In the north (i.e. Liverpool Ranges), the terrain is rugged and accessibility restricted, hence the area remains highly vegetated. To the south (i.e. Merriwa Plateau), clearing has been more extensive as the rolling to hilly terrain ensures greater accessibility. Grazing (sheep and beef cattle) and cropping activities dominate cleared areas, due to the high fertility of basaltic soils. Kovac and Lawrie (1991) classify the region's vegetation as eucalypt tree savannah, with sparse tree cover with grassland communities dominant. Common species include *Austrostipa aristiglumis* (Plains Grass) and various *Poa* (tussock) species.

3. Methods

3.1. Field sampling

Field sampling was undertaken on three separate sampling campaigns in 2006, 2014 (Krui catchment) and 2015 (Merriwa catchment). The Krui 2006 campaign sampled across 41 sites, which were resampled in June–July 2014 (Fig. 4). The Merriwa 2015 campaign

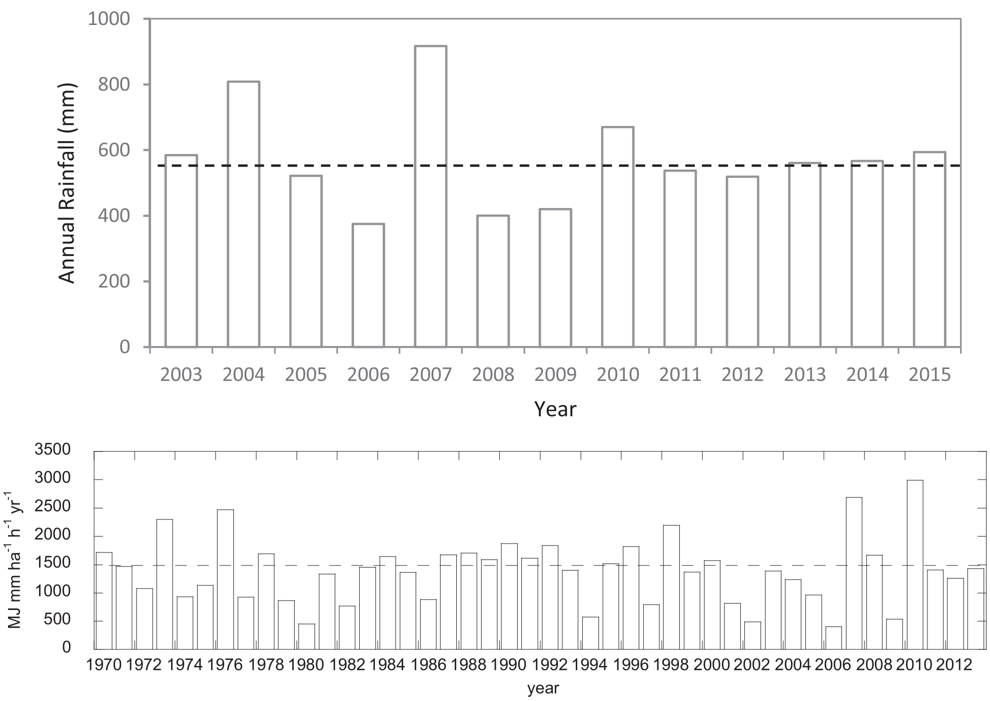

Fig. 3. Cumulative rainfall (mm) for 2003–2015 across the Krui and Merriwa catchments (top). The dashed line shows the average annual rainfall from 2003 to 2015. The bottom figure represents rainfall erosivity as calculated by the method of Renard and Freimund (1994) for the entire Roscommon weather station site record (www.bom.gov.au). Of particular note is the high rainfall and high rainfall erosivity years of 2007 and 2010 which are the largest on record since the station opened in 1969.

sampled 47 sites. The data is summarised in Table 2.

Location of sample sites and sampling coordinates were organised prior to sampling based on an approximate 1 km grid scale across the catchments. The location of the sites was examined for accessibility using topographical maps and Google Earth images with the goal to collect all samples in open grassland. Sites close to trees were moved to a distance of at least 50 m from trees to avoid their influence. Locations in the field were also adjusted where necessary, based on land use change or site accessibility, with the locations of sample sites recorded with a Global Positioning System (GPS) device. The resultant sample pattern was a compromise between accessibility, site practicability, and time, resulting in the sampling distribution in Fig. 4.

No samples were collected in the southern end of the Krui or Merriwa catchments due to the different (sedimentary) geology and resultant sandstone derived soils located there. Hence, for consistency, soil samples in the Krui and Merriwa catchments were kept to basalt-derived soils and pasture (grazing) sites.

3.2. Field sampling and lab analysis

Field sampling is always a compromise between the number of samples and the time required to collect them, which ultimately determine the final cost. Other studies have sampling densities ranging from 0.002 to over 1100 samples per km^2 (Minasny et al., 2013). Here we adapted the method of Minasny et al. (2013) who show that the grid size (resolution) of digital maps increase logarithmically with spatial extent, and the grid size decreases logarithmically with sampling density. The study sites here (Krui's extent of 562 km^2 and Merriwa of 606 km^2) were close to the trend-line and comparable to other studies of similar sampling density (Minasny et al., 2013) (Fig. 5). Therefore, sampling density is in keeping with other studies.

At each sample location, two soil cores were collected adjacent to each other. The samples were 210 mm (deep) and 110 mm (shallow) long, both with internal diameters of 94 mm. Deep and shallow cores were collected as different plant functional groups may have different C input rates into soil depending on the depth that soil C is measured. For example, grasses have 44% of their root mass in the top 10 cm of soil (Jackson et al., 1996). Further, previous work also indicated that 210 mm captured the entire ^{137}Cs profile (Martinez et al., 2009; Hancock et al., 2018). Therefore, the two sampling depths allowed an assessment of both near surface and rooting depth soil properties.

For sampling, each core was fitted with a steel cap, which allowed the core to be driven into the ground with a sledge hammer. In areas where maximum soil depth was < 210 mm, cores were instead taken to the maximum insertion depth, with depth recorded. Once inserted to the desired depth, cores were removed either by excavation of the core, or by using vice-grips to twist the metal core from the ground. Soil samples were then labelled and double-bagged for transport. Core holes were then infilled to prevent injury to livestock.

In the laboratory, soil samples were weighed, dried in a 40 °C oven, and reweighed after 7 days, or until weight change was < 1%. Coarse (> 2 mm) fractions were disaggregated mechanically and by hand using a mortar and pestle. The samples were then passed through a 2 mm sieve and the mass recorded. Subsamples were sent to the Environmental Analysis Laboratory at Southern Cross University, Lismore, NSW, for total C and total N assessment using the LECO dry combustion method. Soils were analysed for ^{137}Cs as described in Section 3.5 below.

3.3. Topographic data and GIS analysis

Here we used the 25 m Land and Property Information (LPI) New South Wales digital elevation model (DEM) which is derived from digitised 10 m contour and drainage data sourced from the LPI 1:25000 topographic map series. This is the best available digital topographic data for the catchments and is available for most eastern and central regions of New South Wales (Martinez et al., 2010a). The DEM was imported as a raster grid file into the ArcMap platform of the ArcGIS 10.2 program with pit-filling undertaken prior to terrain data being generated to remove potential errors which may remain in the DEM after processing.

3.4. Rainfall data

To examine the influence of rainfall across the Krui and Merriwa catchments, and its potential relationship with SOC, rainfall data was obtained from the Bureau of Meteorology (www.bom.gov.au, site number 61287) and Goulburn Region Experimental Dataset (Rüdiger

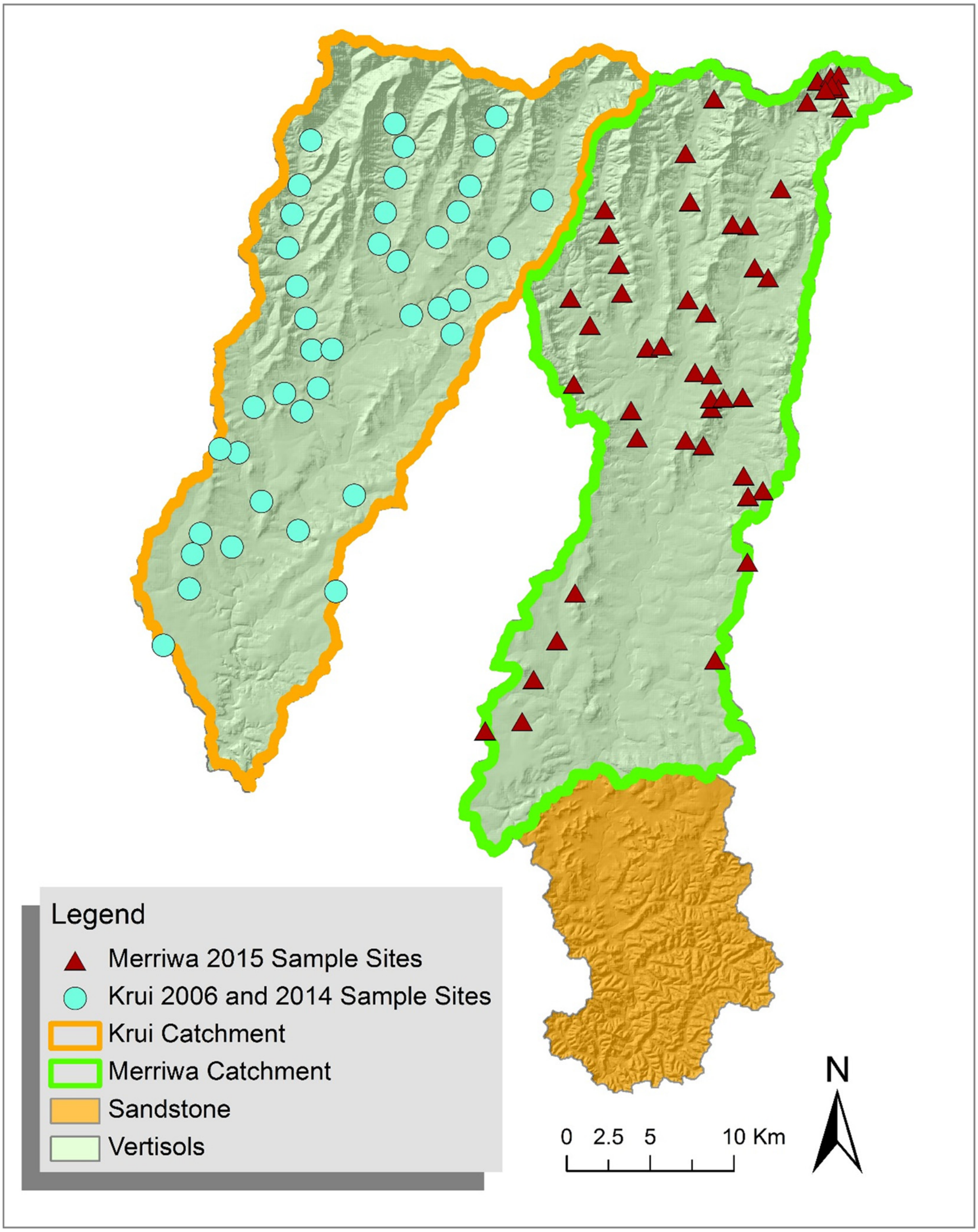

Fig. 4. Location of soil sample sites for Krui 2006, 2014 and Merriwa 2015.

et al., 2007; Kunkel et al., 2016) (Figs. 3 and 6).

3.5. ^{137}Cs analysis

The caesium-137 (^{137}Cs) method has been used globally to determine soil redistribution patterns and quantify soil erosion rates and can be used to infer medium-term (up to 50 year old) soil erosion/deposition behaviour (Loughran, 1994; Walling and He, 2001; Zapata, 2002), and has been successfully employed in the study catchment (Martinez et al., 2009; Hancock et al., 2015). ^{137}Cs is an artificial radioisotope that is a by-product of the atmospheric testing of nuclear weapons. Upon fallout and reaching the earth surface it is rapidly and strongly adsorbed to fine soil particles (silts and clays). Soil movement can be calculated from the accumulation and depletion of ^{137}Cs at a given location relative to levels observed at a nearby non-erosive (reference site). ^{137}Cs has relatively short half-life (30.1 years) and unlike Europe, there has been no additional input since atmospheric testing of nuclear weapons ceased (early 1970s). However, there are still detectable concentrations in many parts of Australia.

Given it is an anthropogenic isotope and is relatively easy to measure, it makes it an ideal soil tracer to qualitatively and quantitatively assess soil redistribution rates (Loughran, 1994; Walling and He, 2001; Zapata, 2002; Krause et al., 2003). For the ^{137}Cs analysis, soil samples (the < 2 mm soil fraction with a mass between 400 and 1000 g) were placed in a Marinelli beaker on a hyperpure germanium detector. Sample count times were approximately 86,400 s (i.e. 24 h), with counting errors in the order of +/− 10% or less achieved (one standard deviation). The concentration of ^{137}Cs in the samples was calculated using the equation outlined by Loughran (1994) and Loughran et al. (2002). The method employed here has been well described

Table 2
Descriptive statistics of SOC for the Krui and Merriwa catchments.

	Krui 2006		Krui 2014		Merriwa 2015	
	210 mm	110 mm	210 mm	110 mm	210 mm	110 mm
SOC (%)						
n	41	41	41	41	47	47
Min	1.88	1.78	1.95	2.16	1.77	2.19
Mean	3.33	3.55	3.20	4.04	3.52	4.22
Median	3.27	3.52	3.04	3.67	3.35	4.09
Max	6.89	6.26	6.45	9.29	6.27	8.09
σ	1.13	1.04	0.92	1.45	1.02	1.29
^{137}Cs (mBq g^{-1})						
Min	0.14	0.28	0.59	0.57	0.16	0.77
Mean	1.93	2.58	2.32	3.11	1.75	2.80
Median	1.93	2.71	2.05	2.80	1.70	2.50
Max	4.10	4.61	7.50	7.53	5.20	8.90
σ	0.88	1.19	1.29	1.84	0.88	1.60

elsewhere (Martinez et al., 2009, 2010b; Hancock et al., 2015).

4. Results

4.1. SOC and ^{137}Cs spatiotemporal distribution

Average SOC concentrations for Krui 2006 and Krui 2014 and Merriwa 2015 data were all above the critical minimal threshold limit of 2% for temperate regions required for aggregate stability for both the 210 mm and 110 mm sample depths (Hazelton and Murphy, 2007; Patrick et al., 2013) (Table 2). The 210 mm cores all had lower SOC concentrations than the corresponding 110 mm cores demonstrating that SOC is concentrated in the near surface.

At the catchment scale there was no significant difference between the Krui 2006 and 2014 210 mm SOC data sets suggesting that there was no change in SOC at the catchment scale over this period (Table 2). However, there was a difference between the Krui 2006 and 2014 110 mm cores with the 2014 data being significantly higher. There was no difference between the Krui 2014 and Merriwa 2015 210 mm or the Krui 2014 and Merriwa 2015 110 mm SOC data sets suggesting that at the catchment scale SOC is very similar despite the one year difference in sample collection timing.

In terms of spatial distribution and relationship with topography, SOC significantly increases with elevation for the 210 mm data sets (Krui 2006 $r = 0.43$, $p < 0.05$; Krui 2014 $r = 0.57$, $p < 0.001$; Merriwa 2015 $r = 0.56$, $p < 0.001$) as well as the 110 mm data sets (Krui 2006 $r = 0.41$, $p < 0.01$; Krui 2014 $r = 0.61$, $p < 0.001$; Merriwa 2015 $r = 0.56$, $p < 0.001$) (Fig. 7).

There is no acceptable or ideal ^{137}Cs concentration for soils (as concentration depends on atmospheric fallout, site conditions and past and present management), however all samples had detectable levels of ^{137}Cs (Table 2). Here all values have been corrected for radioactive decay to 2005 for comparison with other field data collected in the region (Martinez et al., 2009, 2010b; Hancock et al., 2015). For both the Krui and Merriwa soils the 210 mm data had a consistently lower ^{137}Cs concentration than the 110 mm data as the deeper soil (which contains less ^{137}Cs) dilutes the overall concentration (Table 2). This is demonstrated in Fig. 8 where the ^{137}Cs is concentrated in the top (approximately) 100 mm for sites in the study region (Martinez et al., 2009, 2010b). At the catchment scale there was no significant difference between the 2006 and 2014 210 mm Krui data ($p = 0.05$) and they were significantly correlated ($r = 0.43$, $p < 0.005$). There was also no significant difference between the 110 mm data and they were also significantly correlated ($r = 0.35$, $p < 0.05$).

A consistent positive trend was found between ^{137}Cs and elevation for all data sets however this was not significant in all cases for the 210 mm (Krui 2006 $r = 0.32$, $p < 0.05$; Krui 2014 $r = 0.25$, $p < 0.10$; Merriwa 2015 $r = 0.57$, $p < 0.001$) and 110 mm sample depths (Krui 2006 $r = 0.31$, $p = 0.06$; Krui 2014 $r = 0.48$, $p < 0.005$; Merriwa 2015 $r = 0.65$, $p < 0.001$) (Fig. 9).

Strong and significant correlations were found between SOC and ^{137}Cs for all data sets for both the 210 mm (Krui 2006 $r = 0.57$, $p < 0.001$; Krui 2014 $r = 0.71$, $p < 0.001$; Merriwa 2015 $r = 0.70$, $p < 0.001$) and 110 mm sample depths (Krui 2006 $r = 0.53$, $p < 0.001$; Krui 2014 $r = 0.75$, $p < 0.001$; Merriwa 2015 $r = 0.56$, $p < 0.001$) (Fig. 10). The results suggest that SOC is related to both elevation and to erosion and deposition patterns as demonstrated by the correlation with ^{137}Cs concentrations. Therefore, a low ^{137}Cs concentration indicates erosion and a loss of SOC. Conversely, a high ^{137}Cs concentration suggests deposition and an increase in SOC.

However, this finding may be confounded by two issues (1) rainfall increases moving up the catchment (Fig. 6) which will likely result in higher ^{137}Cs fallout (Walling and He, 2001); and (2) increased rainfall is likely to result in more vegetation which may lead to increased C inputs and therefore higher SOC concentrations. Therefore, the findings here may be serendipitous. This is examined further below (Section 4.2).

No relationships were found between ^{137}Cs concentration and SOC with topographic factors such as slope gradient (%), curvature and upslope contributing area, for any of the data sets. This suggests that the catchment scale patterns of soil redistribution were not influenced by topographic factors. Others have found similar results for grassland sites (Kaste et al., 2006; Nearing et al., 2005; Martinez et al., 2009;

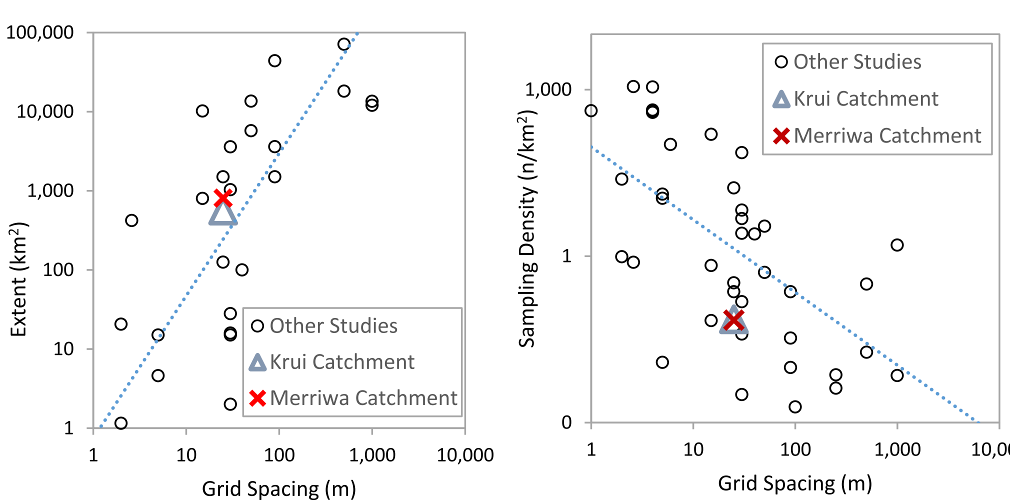

Fig. 5. Relationship between DEM grid size and extent of the study site (left), and the relationship between sample density and grid size of the DEM (right).

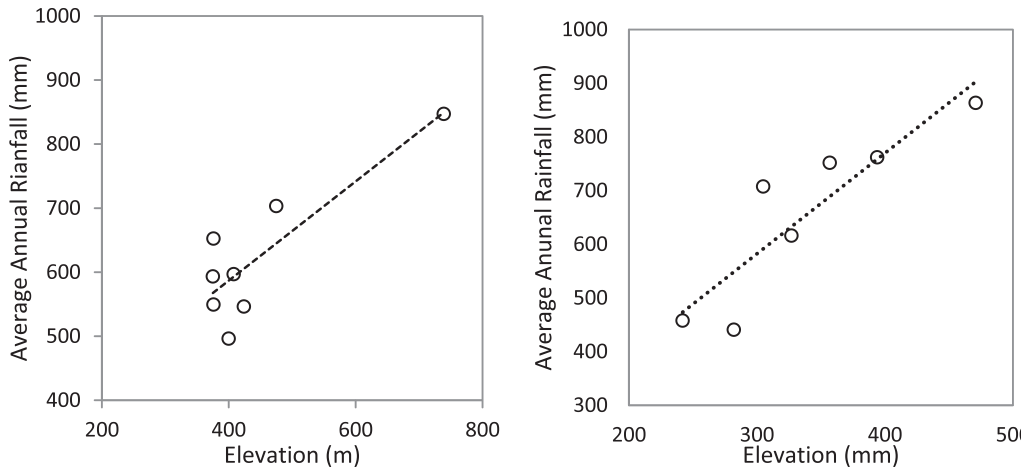

Fig. 6. Elevation versus rainfall from the Krui catchment weather stations K1 to K6, and BOM site "Roscommon" (61287) (left). Elevation versus rainfall based on Merriwa catchment weather stations M1 to M7, and BOM site "Terragong" (61073) (right).

Hancock et al., 2010b).

4.2. Soil erosion assessment and temporal change

To determine an erosion rate using the ^{137}Cs method involves a comparison of ^{137}Cs inventory measured at the study site against that measured at a reference site, with large spatial scales requiring multiple ^{137}Cs reference sites (such as the catchments examined here) (Loughran, 1994; Walling and He, 2001; Zapata et al., 2002; Kirchner, 2013). This is due to differences in the ^{137}Cs uptake in different soils with varying clay content as well as differences in rainfall amount and distribution that influence the initial ^{137}Cs fallout (Zapata, 2002; Kirchner, 2013). In the catchments examined here, rainfall has been shown to vary considerably as elevation increases (Fig. 6). Therefore, it is very likely that the ^{137}Cs reference inventory will vary with rainfall up the Krui and Merriwa elevation gradient and that multiple inventories would be needed to determine erosion rates. Fig. 8 demonstrates this point using depth increment sampling at relatively low rainfall at the base of the catchment (Stanley 350 m elevation, Martinez et al., 2009), versus high rainfall at the top of the catchment (Spring Hill, site K6–720 m elevation) (Hancock et al., 2018) with differences in both total ^{137}Cs concentration and depth distribution evident.

Although sampling multiple reference ^{137}Cs locations for the entire study site and along the rainfall gradient is technically possible, it is well beyond the scope of this project for catchments of this size (two catchments with total area > 1500 km^2). Here we use the temporal change in ^{137}Cs (Δ^{137}Cs) for the individual Krui sample sites (after adjusting for radioactive decay), to determine if individual sites were erosional ($\Delta^{137}Cs > 0$), depositional ($\Delta^{137}Cs < 0$), or at equilibrium ($\Delta^{137}Cs \approx 0$). Hence, Δ^{137}Cs was used to represent erosional and depositional processes across individual sample sites between 2006 and 2014.

To determine the influence of erosion and deposition on SOC for individual sample sites, Δ^{137}Cs was compared to ΔSOC, with ΔSOC calculated in the same way as Δ^{137}Cs, where the 2006 SOC value was subtracted from the Krui 2014 SOC value for each sample site (Fig. 11). The results demonstrate that ΔSOC had a significant relationship with Δ^{137}Cs for both the 210 mm ($r = 0.36$, $p < 0.02$) and 110 mm cores ($r = 0.41$, $p < 0.01$). As Δ^{137}Cs represents a change in the erosion-deposition processes between 2006 and 2014, this indicates that erosion-deposition processes may have been different for the sample sites over the period. Similarly, ΔSOC also represents change of SOC at sample sites between 2006 and 2014. The ΔSOC-Δ^{137}Cs relationship suggests that sample sites with positive Δ^{137}Cs concentrations are associated with areas of deposition, and also had positive ΔSOC concentrations indicating that SOC had accumulated. Similarly, sample sites with negative Δ^{137}Cs concentrations, associated with areas of erosion, also had negative SOC concentrations or lost SOC. However, given the recognised variability in SOC and ^{137}Cs, this result may be serendipitous. Further probabilistic assessment of this ΔSOC-Δ^{137}Cs relationship is discussed below (Section 4.3).

4.3. Probability assessment of soil erosion and temporal change

At issue here is that the above results are determined from a single sample (either 210 mm or 110 mm deep core) collected at a single point. It is well recognised that there is considerable variability in soil physical and chemical properties at short length scales. In particular, both ^{137}Cs and SOC can have considerable point scale variability (Loughran, 1994; Walling and He, 2001; Loughran et al., 2002, 2004; Zapata et al., 2002; Martinez et al., 2009). Therefore, there is the possibility that the above relationships may have occurred due to chance or serendipitous circumstances.

To address this using a field based approach requires multiple soil samples (for ^{137}Cs seven or more cores are usually collected at a point for control values to be determined) at the same depth to be collected (Loughran, 1994; Walling and He, 2001; Loughran et al., 2002; Zapata et al., 2002). However, given the required number of samples and the time and cost involved to obtain, process and analyse an increased number of samples, this approach is beyond the scope and resources of most research teams at the scale examined here.

However, we can use a statistical approach to assess the variability in ^{137}Cs and SOC to test the robustness of the ΔSOC-Δ^{137}Cs relationship. Previous work in the Krui and Merriwa catchments has found that the coefficient of variation of ^{137}Cs is approximately 15% for grassland sites (Martinez et al., 2009; Hancock et al., 2018). Interestingly, the coefficient of variation of SOC at the Stanley site (Martinez et al., 2009) and other grassland sites was also approximately 15%.

We use this defined variability of both ^{137}Cs and SOC to assess the veracity of the above results using a Monte Carlo type approach. Here we created 100 data sets of the Krui 2006 and 2014 ^{137}Cs data using a random variability of 15%. This process was repeated for the 2006 and 2014 SOC data.

For all 100 data sets there were significant relationships between SOC and elevation ($p < 0.05$) (as found for the field data) demonstrating the previous findings are robust. ΔSOC-Δ^{137}Cs was then calculated for each of the 100 data sets and all were found to be significant ($p < 0.05$) suggesting that findings using the single field value are robust. To further evaluate the strength of these findings, the coefficient of variation was increased to 20% with the majority (80%) of the ΔSOC-

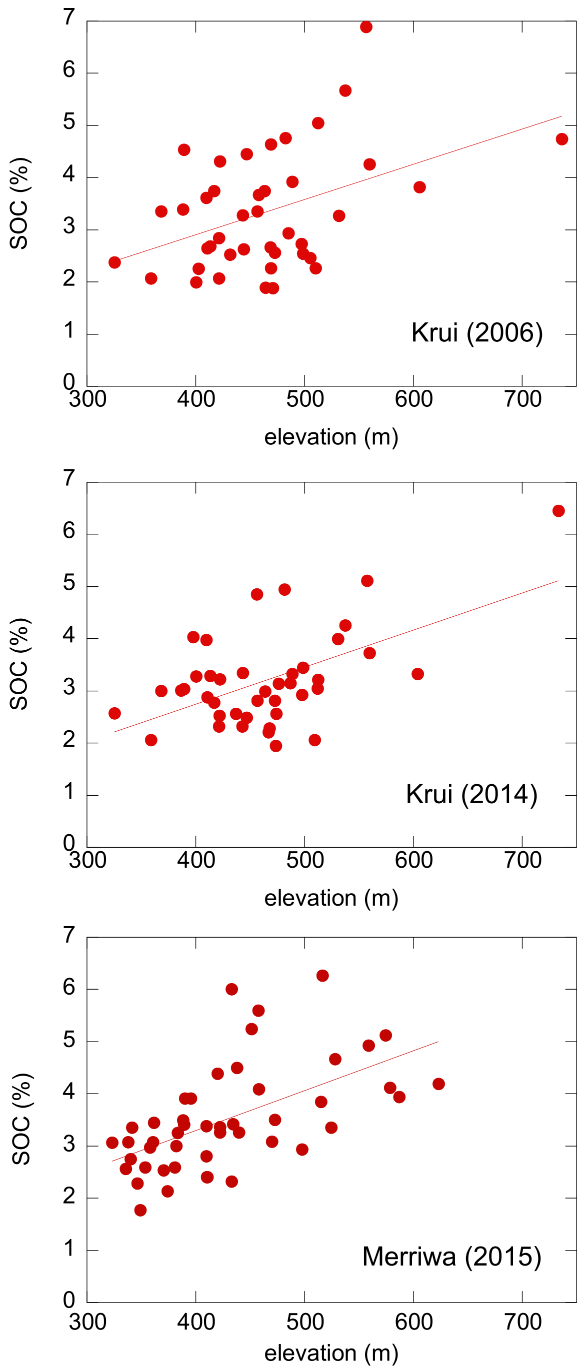

Fig. 7. SOC % (210 mm cores) and elevation (m) for the Krui in 2006 (top), 2014 (middle) and Merriwa (2015) bottom. Fitted regression line included for clarity. Here we only display the 210 mm data for brevity as the 110 mm core data is very similar.

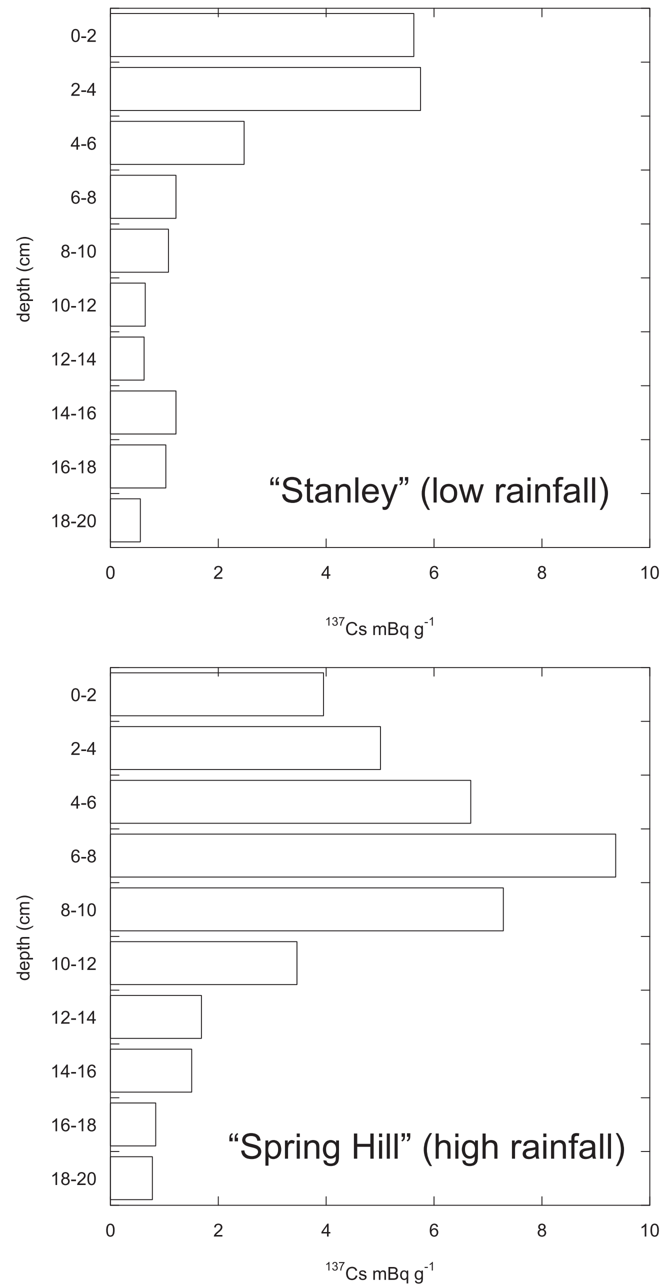

Fig. 8. Depth increment ^{137}Cs profiles for the Krui catchment at lower rainfall (Stanley property; Martinez et al. (2009)) (top) and higher rainfall area (Spring Hill – Site K6, Table 1) (bottom). The data demonstrates that for the study area and soils examined here the majority of ^{137}Cs is concentrated in the top 20 cm of the soil profile.

Δ^{137}Cs relationships significant. This error based approach suggests that there has been a demonstrable change in ^{137}Cs and SOC across the catchment.

This assessment was only performed for the Krui catchment 210 mm data as we do not have variability data for ^{137}Cs or SOC for 11 cm soil depth. Nor do we have repeat field data for the Merriwa catchment.

5. Discussion

There is considerable speculation on how SOC will respond to changing climate, in particular, to any change in rainfall amount and intensity (Lal, 2001, 2003; Kirkels et al., 2014; Doetterl et al., 2016; Poesen, 2018). Quantifying soil erosion and deposition in relation to SOC is a non-trivial task. The use of environmental tracers (here ^{137}Cs) offer a field based method that can be employed at the large catchment scale. Implicit in this analysis has been sources of error and repeatability by use of the same sites at different times as well as using both erosional and depositional change in relation to SOC (De Vente et al., 2007; Parsons and Foster, 2011). We have also examined the results using a probabilistic (Monte-Carlo type) approach. The findings here indicate that there has been a significant change in SOC over an approximately eight year period.

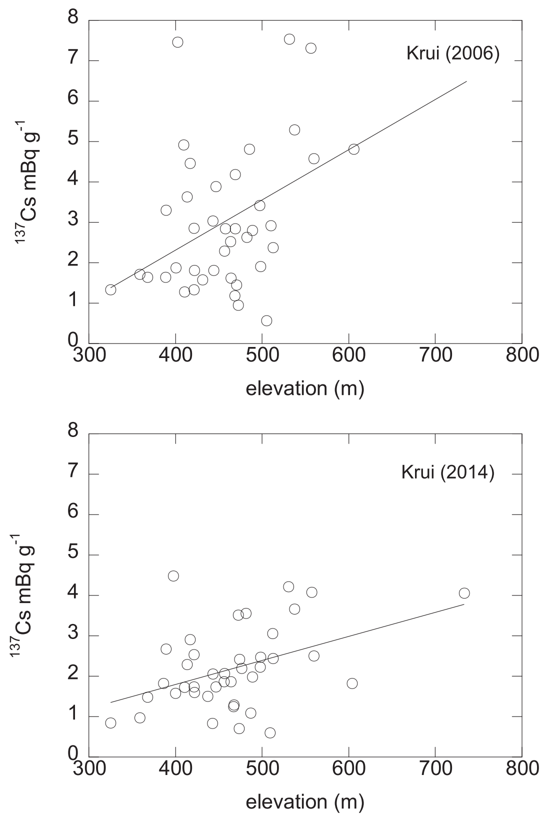

Fig. 9. Relationship between elevation and ^{137}Cs for the Krui in 2006 (top) and 2014 bottom. Here we only display the 210 mm data for brevity as the 110 mm core data is very similar.

5.1. *Large catchment-scale spatiotemporal distribution of SOC*

Several other authors have found a relationship between SOC and elevation (Minasny et al., 2013; Kunkel et al., 2019). However, elevation itself is not the direct physical cause of SOC distribution as it may be influenced by orographic precipitation, with precipitation increasing as elevation increases. A precipitation gradient influences vegetation growth and density, with a concomitant influence on SOC cycling (Fig. 1). Hence, at the large catchment-scale here, climate or orographic rainfall controls SOC. Elevation can therefore be used as a surrogate for the influence of rainfall on SOC in this environment (Kunkel et al., 2019).

Although the elevation-rainfall gradient is suggested to be a potential driver of SOC, catchment average SOC was temporally stable, as shown by the lack of significant difference between Krui 2006 and Krui 2014 SOC at the catchment scale. The period from 2002 to 2010 was known as the Millennium Drought (Mills et al., 2010; Verdon-Kidd et al., 2014). Therefore, SOC may have been expected to be reduced as a result of less rainfall supporting less vegetation growth. At the catchment scale this does not appear to be the case in this study. This suggests that long-term, seasonal variability in climate may require drastic changes to cause short term (less than decadal) changes in SOC concentration.

Although there was no significant difference in SOC sampled eight years apart, there is the possibility that SOC fluctuated between each sampling. Future research may require regular two to five-year sampling of the catchments. However, unpublished SOC data collected every two years at a grassland site in the lower Krui suggests that there has been no change in SOC from 2005 to present. Based on the lack of SOC analysis at large catchment-scales, the continued uncertainty of carbon cycle feedbacks, and the complexity of interactions of controls on and transport of soil C, further investigation into SOC

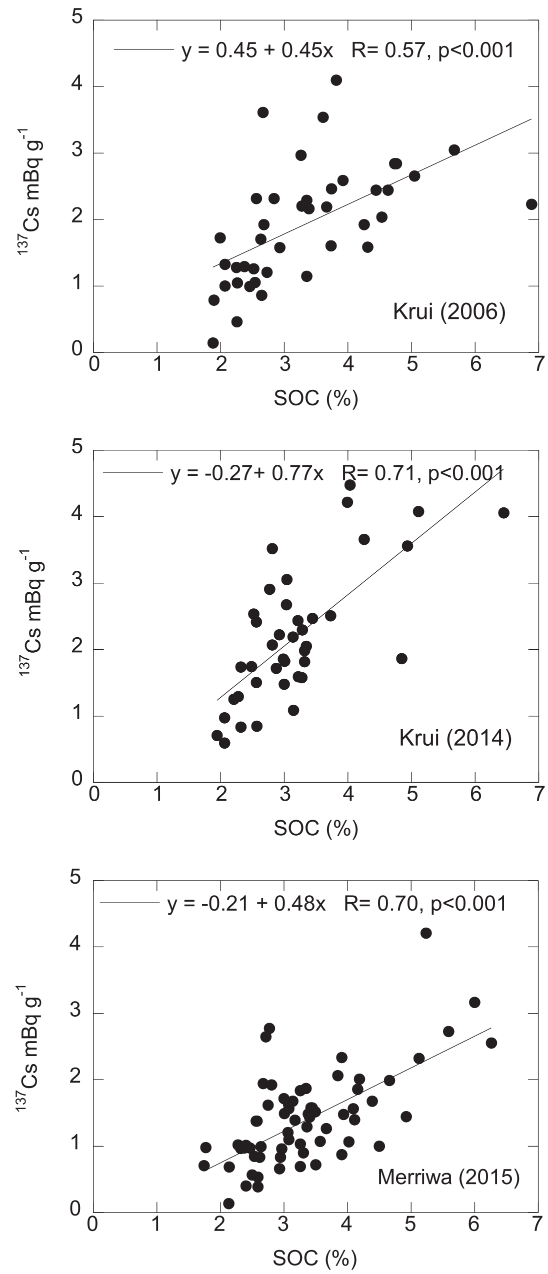

Fig. 10. SOC % and ^{137}Cs mBq g^{-1} (210 mm cores) for the Krui in 2006 (top), 2014 (middle) and Merriwa (2015) bottom.

spatiotemporal distribution is justified (i.e. regular and repeat sampling at the same locations). This would create a valuable, spatiotemporal dataset of SOC dynamics.

5.2. *Soil redistribution rates and climate*

To calculate an erosion rate using conventional methods as described by Walling and He (2001) and Zapata et al. (2002) was not possible for this study. The use of ^{137}Cs as a surrogate for the erosion and deposition across the study site, requires multiple ^{137}Cs reference sites along the rainfall gradient and was not feasible. Instead, Δ^{137}Cs between 2006 and 2014 was used to represent erosion and deposition at individual study sites.

While the ^{137}Cs method is conceptually straightforward, practically it is quite complex. Consequently there are a lack of studies where the analysis process is repeated at the same positions (Loughran and Balog,

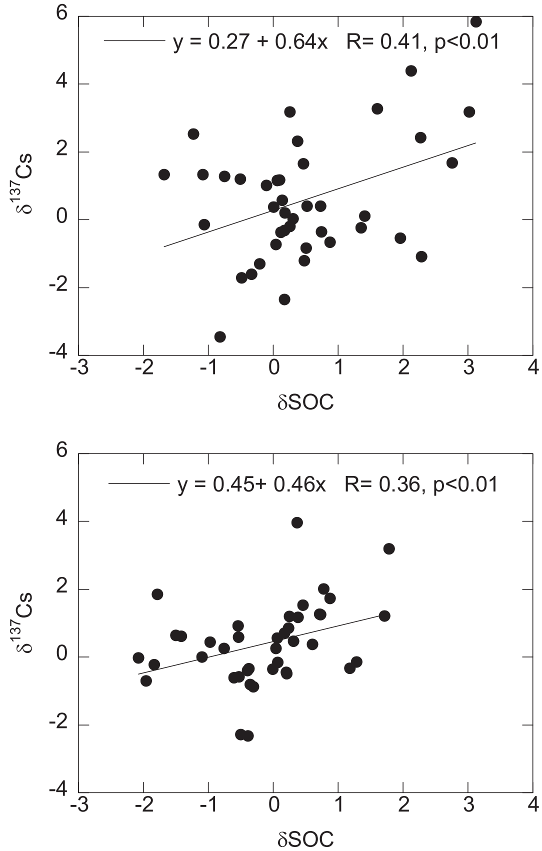

Fig. 11. ΔSOC and Δ^{137}Cs for the 110 mm (top) and 210 mm cores (bottom).

2006; Hancock et al., 2015). The work here demonstrates that erosion and deposition has changed at the catchment scale (over an eight year period). This suggests that there has been a major erosional event in the catchment.

Rainfall records demonstrate that since 2006 there were two years when rainfall was well above average (2007–886 mm; 2010–947 mm) (Fig. 3). In particular, in 2007 there was a major rainfall event of 117 mm that occurred with a maximum hourly rainfall of 48 mm. This was the largest event since 1969 (Merriwa-Roscommon, station number 61287 was opened in 1969) (Mills et al., 2010; Verdon-Kidd et al., 2014). The storm is colloquially known as the 'Pasha Bulka storm' after the bulk carrier that beached itself just outside the port of Newcastle. The year 2010 was also a high rainfall year, however, there were no intense events. Rainfall erosivity as calculated using the method of Renard and Freimund (1994) (Fig. 3) demonstrates that erosivity was the highest on record in 2007 and 2010. Field observations by the authors confirm that severe erosion (sheet and gully erosion) was observed in 2007. A further point to note is this rainfall event occurred at the end of a multi-year drought period where vegetation was minimal (Verdon-Kidd et al., 2014). There was no severe erosion observed in 2010. Further evidence for the impact of the 2007 event is provided by numerical modelling (using a numerical model, CAESAR) where Hancock and Coulthard (2012) demonstrated that the 2007 rainfall was likely to have been a geomorphically significant event. Therefore we believe that the 2007 event was the driver of the findings here.

5.3. Determining SOC redistribution

There was a significant relationship between Δ^{137}Cs and ΔSOC which indicates that erosion and deposition processes influenced the temporal change in SOC distribution for individual sample sites. The ΔSOC-Δ^{137}Cs relationship suggests that sample sites with positive Δ^{137}Cs concentrations (associated with areas of deposition), correlated with positive ΔSOC concentrations, or an increase in SOC. Similarly, sample sites with negative Δ^{137}Cs concentrations, associated with areas of erosion, had negative ΔSOC concentrations, or a decrease in SOC. While catchment average SOC concentrations were not significantly different between 2006 and 2014, the significant relationship between ΔSOC and Δ^{137}Cs indicated SOC redistribution was occurring across individual sites. The Monte-Carlo assessment of the point scale data confirms these results.

The significance of the SOC-Δ^{137}Cs relationship suggests that there was a strong erosional-deposition event or events to affect such a change - with rainfall intensity a dominant factor controlling erosion processes (Zhao et al., 2015). Hence, the change in both Δ^{137}Cs and ΔSOC from 2006 to 2014 is attributed to the high intensity rainfall event of 8-9th June 2007. Similar, high intensity events in the future may thus see further changes in SOC distribution across the catchment.

While we take a catchment scale approach here over a limited time period and focus on soil erosion and deposition, increased storm frequency and intensity as well as increased temperature will influence biogeochemical cycles and SOC cycling. There is a need for fully coupled catchment scale models which can assess the impact of changing climate and the C store so that society can better manage both our agricultural and natural landscape systems (Quinton et al., 2010; Doetterl et al., 2015; Wells et al., 2013; Wells and Hancock, 2014). Models will be the only method that will allow an assessment of both hillslope and climate as well as integrate feedbacks to understand future change.

5.4. Study limitations and future work

This work highlights how repeat sampling at the same sites can provide insight into biophysical processes and, in particular here, landscape response to an extreme event. The approach using environmental tracers provides a method by which the impacts of an extreme event can be assessed in terms of erosion and deposition. Other methods to measure erosion and deposition such as hillslope sediment traps and erosion pins are not practical over such large areas as this or in areas which are privately owned and subject to cattle grazing (which can and do destroy instruments!).

Other environmental tracers such as ^{210}Pb and ^{7}Be can also be employed to explore both short and longer-term erosion and deposition patterns. ^{7}Be (half-life ~ 53 days) in particular may be useful to assess storm events while ^{210}Pb may provide insights into longer-term patterns (Zapata, 2002; Zapata et al., 2002). Use of these tracers will be the focus of future work.

While storm events such as that examined here occur infrequently, it is important that background data be available with which to evaluate landscape response. Such long-term monitoring data is invaluable to better understand both the natural and agricultural environments and also quantify the C and sediment fluxes. Here, given the catchment is ungauged and there is no water quality data we can make no comment on how much C is exported annually or by the 2007 storm and 2010 high rainfall year. Our data only allows us to assess hillslope scale redistribution. Quantification of the C flux through the hydrological network is required to determine a catchment scale C balance. The results here show no change in average SOC at the catchment scale however there is strong evidence for an internal reorganisation.

The findings here are for a single catchment and for a single major rainfall event. It is important that other sites with different topography, soils and landscape management be assessed. Unfortunately, we do not have repeat data for the Merriwa catchment. However, given the geomorphic similarity and the same SOC and ^{137}Cs trends we believe the soil erosion and SOC movement and patterns would be similar. If we are to better adapt to climate change then this long-term and large-scale catchment information is vital. The technique employed here can easily be employed elsewhere. Therefore, long-term study sites should be established in key areas. Having long-term monitoring data allows us to have robust information, which will allow us to quantify the effects of significant climate events on soils and geomorphology. Without field data we are left to use models and speculation.

6. Conclusion

Here we examine SOC distribution and soil erosion and deposition patterns across two large geomorphologically similar catchments. Such large scale and relatively high resolution data is rare in the literature. The results show that when comparing SOC change at each point with a measure of erosion and deposition using an environmental tracer (^{137}Cs) there is strong evidence that SOC has been redistributed. The results suggest that change in SOC can be related to erosion and deposition patterns and we attribute this to a single large rainfall event. The findings suggest that a large storm event can influence SOC concentration at the large catchment scale. While the large rainfall event occurred during a prolonged drought when vegetation was likely to be minimal, an increase in the length of dry periods (i.e. increased drought frequency) and an increase in storms (as predicted by some climate models for this part of Australia) may increase the movement of SOC.

Acknowledgements

Special thanks are given to the landholders of the Krui and Merriwa catchments for their cooperation and hospitality. This research was largely supported by Australian Research Council Discovery Grants (DP 0556941: "Carbon, nutrient and sediment dynamics in a semi-arid catchment" and DP110101216: "A next generation spatially distributed model for soil profile dynamics and pedogenesis incorporating soil geochemistry and organic matter"). Professor Des Walling is thanked for advice and support in regards to the ^{137}Cs analysis. The anonymous reviewers are thanked for the supportive and helpful comments. The authors have no conflict of interest.

References

Australian Bureau of Meteorology, 1988. Climatic Atlas of Australia. Australian Government Printing Service, Canberra, Australia.

Berhe, A.A., Harte, J., Harden, J.W., Torn, M.S., 2007. The significance of the erosion-induced terrestrial carbon sink. Bioscience 57, 337–346. https://doi.org/10.1641/B570408.

Berhe, A.A., Harden, J.W., Torn, M.S., Harte, J., 2008. Linking soil organic matter dynamics and erosion-induced terrestrial carbon sequestration at different landform positions. J. Geophys. Res. 113. https://doi.org/10.1029/2008JG000751.

Berhe, A.A., Arnold, C., Stacy, E., Lever, R., McCorkle, E., Araya, S.N., 2014. Soil erosion controls on biogeochemical cycling of carbon and nitrogen. Nat. Ed. Knowl. 5 (8), 2.

Chen, M., Willgoose, G.R., Saco, P.M., 2015. Evaluation of the hydrology of the IBIS land surface model in a semi-arid catchment. Hydrol. Process. 29, 653–670. https://doi.org/10.1002/hyp.10156.

CSIRO, 2016. State of the Climate. 2016. https://www.csiro.au/en/Showcase/state-of-the-climateCSIRO, CSIRO, Australia.

De Vente, J., Poesen, J., Mahmood, A., Verstraeten, G., 2007. The sediment delivery problem revisited. Prog. Phys. Geogr. 31 (2), 155–178. https://doi.org/10.1177/0309133307076485.

Doetterl, S., Six, J., Van Wesemael, B., Van Oost, K., 2012. Carbon cycling in eroding landscapes: geomorphic controls on soil organic C pool composition and C stabilization. Glob. Chang. Biol. 18 (7), 2218–2232. https://doi.org/10.1111/j.1365-2486.2012.02680.x.

Doetterl, S., Stevens, A., Six, J., Merckx, R., Van Oost, K., Casanova Pinto, M., Casanova-Katny, A., Munoz, C., Boudin, M., Zagal Venegas, E., Boeckx, P., 2015. Soil carbon storage controlled by interactions between geochemistry and climate. Nat. Geosci. 8 (10), 780–783.

Doetterl, S.S., Asmeret, A., Nadeuc, E., Wang, Z., Sommer, M., Fiener, P., 2016. Erosion, deposition and soil carbon: a review of process-level controls, experimental tools and models to address C cycling in dynamic landscapes. Earth Sci. Rev. 154, 102–122. https://doi.org/10.1016/j.earscirev.2015.12.005.

Dorji, T., Odeh, I.O.A., Field, D.J., Baillie, I.C., 2014. Digital soil mapping of soil organic carbon stocks under different land use and land cover types in montane ecosystems, eastern Himalayas. For. Ecol. Manag. 318, 91–102. https://doi.org/10.1016/j.foreco.2014.01.003.

Fissore, C., Dalzell, B., Berhe, A., Voegtle, M., Evans, M., Wu, A., 2017. Influence of topography on soil organic carbon dynamics in a Southern California grassland. Catena 149, 140–149. https://doi.org/10.1016/j.catena.2016.09.016.

Gregorich, E.G., Greer, K.J., Anderson, D.W., Liang, B.C., 1998. Carbon distribution and losses: erosion and deposition effects. Soil Tillage Res. 47, 291–302. https://doi.org/10.1016/S0167-1987(98)00117-2.

Hancock, G.R., Coulthard, T.J., 2012. Channel movement and erosion response to rainfall variability in southeast Australia. Hydrol. Process. 26, 663–673. https://doi.org/10.1002/hyp.8166.

Hancock, G.R., Lowry, J.B.C., 2015. Hillslope erosion measurement—a simple approach to a complex process. Hydrol. Process. https://doi.org/10.1002/hyp.10608.

Hancock, G.R., Murphy, D., Evans, K.G., 2010a. Hillslope and catchment scale soil organic carbon concentration: an assessment of the role of geomorphology and soil erosion in an undisturbed environment. Geoderma 155, 36–45. https://doi.org/10.1016/j.geoderma.2009.11.021.

Hancock, G.R., Coulthard, T.J., Martinez, C., Kalma, J.D., 2010b. An evaluation of landscape evolution models to simulate decadal and centennial scale soil erosion in grassland catchments. J. Hydrol. https://doi.org/10.1016/j.jhydrol.2010.12.002.

Hancock, G.R., Coulthard, T.J., Martinez, C., Kalma, J.D., 2011. An evaluation of landscape evolution models to simulate decadal and centennial scale soil erosion in grassland catchments. J. Hydrol. 398, 171–183. https://doi.org/10.1016/j.jhydrol.2010.12.002.

Hancock, G.R., Wells, T., Martinez, C., Dever, C., 2015. Soil erosion and tolerable soil loss: insights into erosion rates for a well-managed grassland catchment. Geoderma 237–238, 256–265. https://doi.org/10.1016/j.geoderma.2014.08.017.

Hancock, G.R., Wells, T., Dever, C., Braggins, M., 2018. Hillslope and point based soil erosion – an evaluation of a landscape evolution model. Earth Surf. Process. Landf. https://doi.org/10.1002/esp.4566. in press.

Hazelton, P., Murphy, B., 2007. Interpreting Soil Test Results: What Do All The Numbers Mean? 2nd edition. CSIRO PUBLISHING, 150 Oxford Street (PO Box 1139), Collingwood VIC 3066, Australia (169pp).

Hoyle, F., O'Leary, R.A., Murphy, D., 2016. Spatially governed climate factors dominate management in determining the quantity and distribution of soil organic carbon in dryland agricultural systems. Sci. Rep. 6, 1–12. https://doi.org/10.1038/srep31468.

Hu, Y., Kuhn, N., 2014. Aggregates reduce transport distance of soil organic carbon: are our balances correct? Biogeosciences 11, 6209–6219. https://doi.org/10.5194/bg-11-6209-2014.

Jackson, R.B., Canadell, J., Ehleringer, J.R., Mooney, H.A., Sala, O.E., Schulze, E.D., 1996. A global analysis of root distributions for terrestrial biomes. Oecologia 108 (3), 389–411.

Jenny, H., 1941. Factors of Soil Formation: A System of Quantitative Pedology. 281 pp. McGraw-Hill, New York.

Kaste, J.M., Heimsath, A.M., Hohmann, M., 2006. Quantifying sediment transport across an undisturbed prairie landscape using cesium-137 and high resolution topography. Geomorphology 76, 430–440. https://doi.org/10.1016/j.geomorph.2005.12.007.

Kirchner, G., 2013. Establishing reference inventories of 137Cs for soil erosion studies: methodological aspects. Geoderma 211–212 (0), 107–115. https://doi.org/10.1016/j.geoderma.2013.07.011.

Kirkels, F.M.S.A., Cammeraat, L.H., Kuhn, N.J., 2014. The fate of soil organic carbon upon erosion, transport and deposition in agricultural landscapes – a review of different concepts. Geomorphology 226, 94–105. https://doi.org/10.1016/j.geomorph.2014.07.023.

Kovac, M., Lawrie, J.W., 1991. Soil Landscapes of the Singleton 1:250 000 Sheet. Soil Conservation Service of NSW, Sydney (456 pp).

Krause, A.K., Loughran, R.J., Kalma, J.D., 2003. The use of caesium-137 to assess surface soil erosion status in a water-supply catchment in the Hunter Valley, New South Wales, Australia. Aust. Geogr. Stud. 41 (1), 73–84.

Kuhn, N.J., 2010. Erosion and climate, nature geoscience. Nat. Publ. Group 3, 738. https://edoc.unibas.ch/dok/A5842641.

Kunkel, V., Wells, T., Hancock, G.R., 2016. Soil temperature dynamics at the catchment scale. Geoderma 273, 32–44. https://doi.org/10.1016/j.geoderma.2016.03.011.

Kunkel, V., Hancock, G.R., Wells, T., 2019. Large catchment-scale spatiotemporal distribution of soil organic carbon. Geoderma 334, 175–185. https://doi.org/10.1016/j.geoderma.2018.07.046.

Lal, R., 2001. Soil degradation by erosion. Land Degrad. Dev. 12 (6), 519–539. https://doi.org/10.1002/ldr.472.

Lal, R., 2003. Soil erosion and the global carbon budget. Environ. Int. 29, 437–450. https://doi.org/10.1016/S0160-4120(02)00192-7.

Lal, R., 2004. Soil carbon sequestration to mitigate climate change. Geoderma 123 (1–2), 1–22. https://doi.org/10.1016/j.geoderma.2004.01.032.

Loughran, R.J., 1994. The use of the environmental isotope caesium-137 for soil erosion and sedimentation studies. Trends Hydrol. 1, 149–167.

Loughran, R.J., Balog, R.M., 2006. Re-sampling for soil-caesium-137 to assess soil losses after a 19-year interval in a Hunter Valley vineyard, New South Wales, Australia. Geogr. Res. 44 (1), 77–86. https://doi.org/10.1111/j.1745-5871.2006.00361.x.

Loughran, R.J., Pennock, D.J., Walling, D.E., 2002. Spatial distribution of caesium-137. In: Zapata, F. (Ed.), Handbook for the Assessment of Soil Erosion and Sedimentation Using Environmental Radionuclides. Kluwer Academic Publishers, Dordrecht, pp. 97–109.

Loughran, R.J., Elliott, G.L., MacFarlane, D.J., Campbell, B.L., 2004. A survey of soil erosion in Australia using caesium-137. Aust. Geogr. Stud. 42 (2), 221–233.

Luo, Z., Wang, E., Sun, O.J., 2010. Soil carbon change and its responses to agricultural practices in Australian agro-ecosystems: a review and synthesis. Geoderma 155 (3–4), 211–223. https://doi.org/10.1016/j.geoderma.2009.12.012.

Martinez, C.M., Hancock, G.R., Kalma, J.D., Wells, T., 2007. Spatio-temporal distribution of near surface and root zone soil moisture at the catchment scale. Hydrol. Process. https://doi.org/10.1002/hyp.6869.

Martinez, C.M., Hancock, G.R., Kalma, J.D., 2009. Comparison of fallout radionuclide (caesium-137) and modelling approaches for the assessment of soil erosion rates for

an uncultivated site in south-eastern Australia. Geoderma 151, 128–140. https://doi.org/10.1016/j.geoderma.2009.03.023.
Martinez, C., Hancock, G.R., Kalma, J.D., Wells, T., Boland, L., 2010a. An assessment of digital elevation models (DEMs) and their ability to capture geomorphic and hydrologic properties at the catchment scale. Int. J. Remote Sens. 31 (23), 6239–6257. https://doi.org/10.1080/01431160903403060.
Martinez, C., Hancock, G., Kalma, J., 2010b. Relationships between ^{137}Cs and soil organic carbon (SOC) in cultivated and never cultivated soils: an Australian example. Geoderma 158, 137–147. https://doi.org/10.1016/j.geoderma.2010.04.019.
McBratney, A.B., Santos, M.L.M., Minasny, B., 2003. On digital soil mapping. Geoderma 117, 3–52. https://doi.org/10.1016/S0016-7061(03)00223-4.
Mills, G.A., Webb, R., Davidson, N.E., Kepert, J., Seed, A., Abbs, D., 2010. The Pasha Bulker East Coast Low of 8 June 2007. Tech Rep 23 Centre for Australian Weather and Climate Research, pp. 62.
Minasny, B., McBratney, A.B., Malone, B.P., Wheeler, I., 2013. Digital mapping of soil carbon. Adv. Agron. 118 (3), 4. https://doi.org/10.1016/B978-0-12-405942-9.00001-3.
Minasny, B., Malone, B., McBratney, A.B., Angers, D.A., Arrouays, D., Chambers, A., Chaplote, V., Chen, Z.S., Bhabani, K.C., Dash, S., Field, D.J., Gimona, A., Hedley, C.B., Hong, S.Y., Mandal, B., Marchant, B.P., Martin, M., McConkey, B.G., Winowiecki, L., 2018. Soil carbon 4 per mille. Geoderma 292 (15), 59–86. https://doi.org/10.1016/j.geoderma.2017.01.002.
Moore, I.D., Gessler, P.E., Nielsen, G.A., Peterson, G.A., 1993. Soil attribute prediction using terrain analysis. Soil Sci. Soc. Am. J. 57, 443–452.
Morgan, R.P.C., 2009. Soil Erosion and Conservation. John Wiley & Sons.
Mueller, T.G., Pierce, F.J., 2003. Soil carbon maps contribution no. 01-06-136 from the Kentucky Agricultural Experiment Station, Lexington, KY. Soil Sci. Soc. Am. J. 67 (1), 258–267.
Nadeu, E., Gobin, A., Fiener, P., Wesemael, B.V., Van Ooost, K., 2015. Modelling the impact of agricultural management on soil carbon stocks at the regional scale: the role of lateral fluxes. Glob. Chang. Biol. https://doi.org/10.1111/gcb.12889.
Nearing, M.A., Kimoto, A., Nichols, M.H., Ritchie, J.C., 2005. Spatial patterns of soil erosion and deposition in two small, semiarid watersheds. J. Geophys. Res. 110. https://doi.org/10.1029/2005JF000290.
Oueslati, I., Allamano, P., Bonifacio, E., Claps, P., 2013. Vegetation and topographic control on spatial variability of soil organic carbon. Pedosphere 23 (1), 48–58. https://doi.org/10.1016/S1002-0160(12)60079-4.
Parsons, A.J., Foster, I.D.L., 2011. What can we learn about soil erosion from the use of ^{137}Cs. Earth Sci. Rev. 108, 101–113. https://doi.org/10.1016/j.earscirev.2011.06.004.
Patrick, M., Tenywa, J.S., Ebanyat, P., Tenywa, M.M., Mubiru, D.N., Basamba, T.A., Leip, A., 2013. Soil organic carbon thresholds and nitrogen management in tropical agroecosystems: concepts and prospects. J. Sustain. Dev. 6 (12), 31.
Pennock, D.J., Corre, M.D., 2001. Development and application of landform segmentation procedures. Soil Tillage Res. 58 (3–4), 151–162. https://doi.org/10.1016/S0167-1987(00)00165-3.
Pimentel, D., Harvey, C., Resosudarmo, P., Sinclair, K., 1995. Environmental and economic costs of soil erosion and conservation benefits. Science 267 (5201), 1117. https://doi.org/10.1126/science.267.5201.1117.
Poesen, J., 2018. Soil erosion in the Anthropocene: research needs. Earth Surf. Process. Landf. 43, 64–84. https://doi.org/10.1002/esp.4250.
Poreba, G.J., 2006. Caesium-137 as a soil erosion tracer: a review. Geochronometria 25, 37–46.
Quinton, J.N., Govers, G., Van Oost, K., Bardgett, R.D., 2010. The impact of agricultural soil erosion on biogeochemical cycling. Nat. Geosci. https://doi.org/10.1038/ngeo838.
Renard, K.G., Freimund, J.R., 1994. Using monthly precipitation data to estimate the R-Factor in the revised USLE. J. Hydrol. 157, 287–306. https://doi.org/10.1016/0022-1694(94)90110-4.
Ritchie, J.C., McHenry, J.R., 1975. Fallout Cs-137: a tool in conservation research. J. Soil Water Conserv. 30 (341), 283–286.
Ritchie, J.C., McHenry, J.R., 1990. Application of radioactive fallout cesium-137 for measuring soil erosion and sediment accumulation rates and patterns: a review. J. Environ. Qual. 19 (2), 215–233.
Rüdiger, C., Hancock, G., Hemakumara, H.M., Jacobs, B., Kalma, J.D., Martinez, C., Thyer, M., Walker, J.P., Wells, T., Willgoose, G.R., 2007. Goulburn River experimental catchment data set. Water Resour. Res. 43, W10403. https://doi.org/10.1029/2006WR005837.
Schimel, D., Stephens, B.B., Fisher, J.B., 2015. Effect of increasing CO_2 on the terrestrial carbon cycle. Proc. Natl. Acad. Sci. 112 (2), 436–441. https://doi.org/10.1073/pnas.1407302112.
Story, R., Galloway, R., van de Graff, R., Tweedie, A.D., 1963. General Report on the Lands of the Hunter Valley. Land Research Series 8.
Toy, T.J., Foster, G.R., Renard, K.G., 2002. Soil Erosion: Processes, Prediction, Measurement, and Control. John Wiley & Sons (352pp).
Verdon-Kidd, D.V., Kiem, A.S., Moran, R., 2014. Links between the big dry in Australia and hemispheric multi-decadal climate variability - implications for water resource management. Hydrol. Earth Syst. Sci. 18, 2235–2256. https://doi.org/10.5194/hess-18-2235-2014.
Walling, D.E., He, Q., 2001. Models for Converting 137Cs Measurements to Estimates of Soil Redistribution Rates on Cultivated and Uncultivated Soils, and Estimating Bomb Derived ^{137}Cs Reference Inventories (Including Software for Model Implementation). A Contribution to the IAEA Coordinated Research Programmes on Soil Erosion (D1.50.05) and Sedimentation (F3.10.01). University of Exeter, pp. 32.
Wells, T., Hancock, G.R., 2014. Comparison of vertical transport of 137Cs and organic carbon in agricultural cracking soils. Geoderma 214–215, 228–238. https://doi.org/10.1016/j.geoderma.2013.09.007.
Wells, T., Hancock, G.R., Dever, C., Martinez, C., 2013. Application of RothPC-1 to soil carbon profiles in cracking soils under minimal till cultivation. Geoderma 207–208 (0), 144–153. https://doi.org/10.1016/j.geoderma.2013.05.018.
Zapata, F., 2002. Handbook for the Assessment of Soil Erosion and Sedimentation Using Environmental Radionuclides. Kluwer Academic, Dordrecht, The Netherlands (219pp).
Zapata, F., Garcia-Agudo, E., Ritchie, J.C., Appleby, P.G., 2002. Introduction. In: Zapata, F. (Ed.), Handbook for the Assessment of Soil Erosion and Sedimentation Using Environmental Radionuclides, Chapter 1. Kluwer Academic Publishers, Dordrecht, The Netherlands, pp. 1 13. (pp 219).
Zhao, Q., Li, D., Zhuo, M., Guo, T., Liao, Y., Xie, Z., 2015. Effects of rainfall intensity and slope gradient on erosion characteristics of the red soil slope. Stoch. Env. Res. Risk A. 29 (2), 609–621. https://doi.org/10.1007/s00477-014-0896-1.